J Math Chem (2013) 51:2020–2032
DOI 10.1007/s10910-013-0197-9

ORIGINAL PAPER

Modelling interaction between ammonia and nitric oxide molecules and aquaporins

Hakim Al Garalleh · Ngamta Thamwattana · Barry J. Cox · James M. Hill

Received: 17 January 2013 / Accepted: 23 May 2013 / Published online: 18 June 2013

Abstract Aquaporin is a family of small membrane-proteins that are capable of transporting nano-sized materials. In the present paper, we investigate the structure of these channels and provide information about the mechanism of individual molecules being encapsulated into aquaglyceroporin (GlpF) and aquaporin-1 (AQP1) channels by calculating the potential energy. In particular, we presents a mathematical model to determine the total potential energy for the interaction of the ammonia and nitric oxide molecules and different aquaporin channels which we assume to have a symmetrical cylindrical structure. We propose to describe these interactions in two steps. Firstly, we model the nitrogen atom as a discrete point and secondly, we model the three hydrogen atoms on the surface of a sphere of a certain radius. Then, we find the total potential energy by summing these interactions. Next, by considering the nitric oxide molecule as two discrete atoms uniformly distributed interacting with GlpF and AQP1 channels then gathering all pairs of interaction to determine the potential energy. Our results show that the ammonia and nitric oxide molecules can be encapsulated into both GlpF and AQP1 channels.

Keywords Aquaporins (AQPs) · Aquaporin-1 (AQP1) · Aquaglyceroporin (GlpF) · Ammonia molecule (NH_3) · Nitric oxide (NO) · Lennard-Jones potential · van der Waals interaction

H. Al Garalleh (✉) · N. Thamwattana
Nanomechanics Group, School of Mathematics and Applied Statistics,
University of Wollongong, Wollongong, NSW 2522, Australia
e-mail: hakimqaralleh@hotmail.com

B. J. Cox · J. M. Hill
Nanomechanics Group, School of Mathematical Sciences, University of Adelaide,
Adelaide, SA 5005, Australia

1 Introduction

The aquaporin family comprises at least ten distinct protein channels and are found in all life forms, including mammals, plants and many other organisms [1]. The study of aquaporins (AQPs) has been of considerable interest for nanobiotechnology applications due to the high flow rate and because the interaction of the different molecules inside the AQPs is still not well-understood. The atomic structures of two major members, human aquaporin-1 (AQP1) and aquaglyceroporin (GlpF), have been recently identified [2–4] and the molecular mechanism of passive transport of small neutral solutes passing through these channels has been confirmed through molecular dynamic simulation [5]. The main difference between the two channels is the potential of mean force at the selective filter, where the human AQP1 barrier is larger than that of the GlpF [6,7]. The structural unit of AQP1 is active at a tetramer [8] as shown in Fig. 1, and each monomer has a N- and C-terminal [9] which are joined by a long loop-spanning helix and both terminals compose of three transmembrane-spanning helices [10–12] and the N- and the C-terminus are located on the cytoplasm side of the membrane [12,13]. For more details of the structure of AQP1 protein channel we refer the reader to reference [2]. The residue structure of AQP1 has been confirmed with a length of 3.8 Å [2], while the structure of GlpF, is assessed to be 2.2 Å in length [4,14]. In contrast, the GlpF channel structure follows the directions of three glycerol molecules and two water molecules for each functional unit which has two characteristic

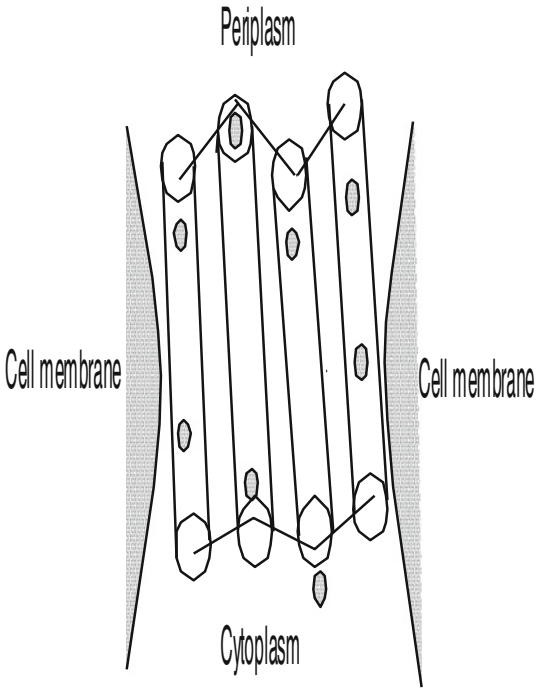

Fig. 1 Structure of monomer unit of the cylindrical aquaporin

half-membrane-spanning which are joined with quasi-two fold symmetry [14]. For more details related to the geometrical structure of the GlpF channel we refer the reader to [2,4,15].

Recently, several studies investigate the molecular selectivity of water channel AQP1 and the GlpF [16]. GlpF and AQP1 channels can facilitate the transport of gases, such as NH_3 and CO_2 across membranes [17]. Phongphanphanee et al. [6] study the permeation of various molecules across AQP1 and GlpF including H_2O, NH_3, CO_2, glycerol and urea [18]. NO has a significant role involving in many physiological and pathological processes in cellular signaling molecule and low levels of nitric oxide are very important to protect the liver from ischemic damage [19]. Either directly or indirectly, ammonia contributes significantly to the nutritional needs of terrestrial organisms as a precursor to food and fertilizers. The potential mean forces (PMFs) have also been computed for the permeation of these biomolecules into AQP1 and GlpF using numerical and computational approaches. The PMFs reported by Phongphanphanee et al. [6] suggest that H_2O and NH_3 can permeate through AQP1 and GlpF while AQP1 has a small activation barrier. De Groot et al. [16] show that the permeation of H_2O and NH_3 has a barrier of 12 kJ/mol. Furthermore, Phongphanphanee et al. [6] suggest that their results are in agreement with experiments results based on the undefined concentration channel while de Groot and coworkers disregard a well-defined membrane region [16]. The work of Verkman [20] indicates that small gas molecules, such as CO_2, NH_3 and NO are transported by proteins should not be ignored [6,18]. Recent experiments show that NH_3 has the potential to pass through GlpF and AQP1 by using different methods, such as the Polymer Reference Interaction Site Model (3D-RISM theory) and the statistical mechanics theory of molecular liquids. The work of Herrera et al. [21] who investigate the NO transport by AQP1 and indicate that NO molecules play a major role in regulating the blood pressure as well as offers an alternate cause for different diseases recently explained by inadequate NO bioavailability. We note that this is the direct evidence that an aquaporin membrane protein facilitates transport of NO and would be an alternate explanation for many diseases, especially hypertension. The water channel AQP-1 are able to transport small gas molecules, such as carbon dioxide, nitric oxide and ammonia in through cell membrane protein [22,23]. To further investigate the mechanism of gases transportation through aquaporin channels, we formulate a mathematical model to determine the potential energy arising from these interactions. In particular, this paper provides the underlying mechanism of ammonia and nitric oxide molecules being encapsulated into the two different types of AQPs. To understand the encapsulation mechanism of biomolecules across cell membranes, this paper investigates the GlpF and AQP1 channels interacting with an ammonia molecule. Here, we apply the discrete-continuum approach and the 6–12 Lennard–Jones potential for the van der Waals interactions in two parts: firstly, we model the nitrogen atom as a discrete point and secondly, the three hydrogen atoms are modelled by a sphere of uniform atomic surface density, each interacting with a flaired right cylindrical GlpF and AQP1 channels with the chemical compositions $C_{1289}H_{2527}N_{315}O_{591}S_{11}$ and $C_{1235}H_{2468}N_{320}O_{601}S_7$, respectively [24]. We perform volume integration throughout the channel to calculate the total interaction potential energy arising from these interactions. We determine analytical expressions for the potential energy, involving series of hypergeometric functions which can be

readily computed using an algebraic computer package, such as MAPLE. Our results show that the ammonia molecule will be accepted into the GlpF and AQP1 channels.

In the next section, we outline the six-twelve Lennard–Jones potential and the methodology for deriving analytical expressions for the potential energy of the various interactions. We obtain the total potential energy arising from the nitrogen atom as a discrete point and a sphere of hydrogen atoms interacting with a flaired right cylindrical aquaporin. Numerical results are presented in Sect. 3. A summary is presented in the final section of the paper.

2 Mathematical model

With reference to Fig. 2, we begin by considering the Lennard–Jones interaction between the aquaporin channel and a discrete point representing a single atom located on the z-axis. Here, the aquaporin channel is assumed to comprise a flaired right cylindrical shape with limited ends. With reference to a rectangular coordinate system (x, y, z), the atom is assumed to be located at $(0, 0, z_0)$ on the z-axis. We introduce the aquaporin channel as a flaired right- cylindrical shell of radius r and centred on the z-axis, parameterized by $(r\delta\cos\theta,\ r\delta\sin\theta,\ z)$, where $\theta \in [-\pi, \pi]$, $z \in [-L/2, L/2]$ and $\delta \in [a, 1]$, where $0 < a < 1$.

The distance ρ between the atom and a typical point in the channel volume is given by

$$\rho^2 = r^2\delta^2 + (z - z_0)^2. \tag{1}$$

$$r = r_0 + 4(r_1 - r_0)(z/L)^2 = r_0 + \alpha z^2, \tag{2}$$

where $\alpha = 4(r_1 - r_0)/L^2$, r_0 and r_1 are the outer radii at the middle and at the opening of aquaporin, respectively. The inner radii at the middle and at the opening of aquaporin are given by ar_0 and ar_1 where $0 < a < 1$ and we take $a = r_0^*/r_0 \approx 0.25$. To find the interaction potential between the single atom and the aquaporin channel, we adopt the Lennard-Jones potential which is given by

$$\phi(\rho) = -A\rho^{-6} + B\rho^{-12} = 4\epsilon\left[-\left(\frac{\sigma}{\rho}\right)^6 + \left(\frac{\sigma}{\rho}\right)^{12}\right], \tag{3}$$

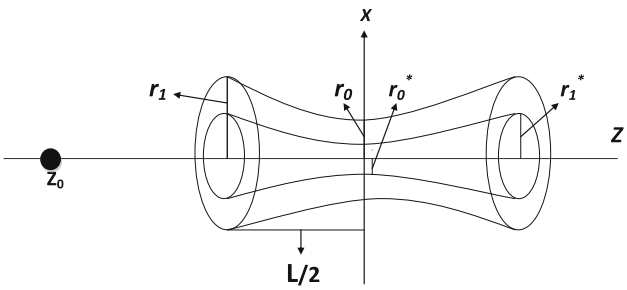

Fig. 2 Geometry of atom on z-axis interacting with an aquaporin assumed to be a flaired right cylinder

where $A = 4\epsilon\sigma^6$ is the attractive constant, $B = 4\epsilon\sigma^{12}$ is the repulsive constant, ϵ is the well depth, σ is the van der Waals diameter. We also use the empirical combining laws [25–27] given by $\epsilon_{12} = (\epsilon_1\epsilon_2)^{1/2}$, and $\sigma_{12} = (\sigma_1 + \sigma_2)/2$, to determine the well depth and van der Waals diameter between different atoms. By summing all pair interactions, the total potential energy of this system can be given by

$$V_{tot} = \sum_i \phi(\rho_i), \tag{4}$$

where ϕ is the potential function given in (3). In the continuum approximation, we may replace this summation by the volume integral, where we assume a uniform atomic density throughout the volume of the aquaporin. Girifalco et al. [28] state that "From a physical point of view the discrete atom-atom model is not necessarily preferable to the continuum mode. We may also use the hybrid discrete-continuum approach". Thus, from (4) we have

$$\begin{aligned} V_{tot} &= \eta_c \int_a^1 \int_{-\frac{L}{2}}^{\frac{L}{2}} \int_{-\pi}^{\pi} \phi(\rho)\, dV \\ &= \eta_c \int_a^1 \int_{-\frac{L}{2}}^{\frac{L}{2}} \int_{-\pi}^{\pi} r^2\delta(-A\rho^{-6} + B\rho^{-12})\, d\delta\, dz\, d\theta\,, \end{aligned} \tag{5}$$

where η_c denotes the atomic density per unit volume and dV is the infinitesimal volume element for the cylindrical aquaporin. We note that the volume element is given by $dV = r^2\delta\, d\delta\, dz\, d\theta$. For detailed analytical evaluation of (5), we refer to the reader to [29].

2.1 Ammonia molecule

In this section, we describe the interaction energy arising from the ammonia molecule encapsulated inside aquaporin channels. We consider the nitrogen atom as a discrete atom interacting with an aquaporin (either GlpF or AQP1) given by

$$V_1 = 2\pi\eta_c \int_a^1 \int_{-\frac{L}{2}}^{\frac{L}{2}} r^2\delta(-A\rho^{-6} + B\rho^{-12})\, d\delta\, dz. \tag{6}$$

The three hydrogen atoms are assumed to be on a spherical shell interacting with the GlpF and AQP1 channels (Fig. 2). From the work of Cox et al. [30], the potential energy of a sphere of the three hydrogen atoms is given by

$$V_2 = \eta_s \pi b \int\int\int \left[\frac{A_H}{2} \left(\frac{1}{\rho(\rho+b)^4} - \frac{1}{\rho(\rho-b)^4} \right) - \frac{B_H}{5} \left(\frac{1}{\rho(\rho+b)^{10}} - \frac{1}{\rho(\rho-b)^{10}} \right) \right] dV$$

$$= \eta_s \pi b \int_a^1 \int_{-\frac{L}{2}}^{\frac{L}{2}} \int_{-\pi}^{\pi} \left[\frac{A_H}{2} \left(\frac{1}{\rho(\rho+b)^4} - \frac{1}{\rho(\rho-b)^4} \right) - \frac{B_H}{5} \left(\frac{1}{\rho(\rho+b)^{10}} - \frac{1}{\rho(\rho-b)^{10}} \right) \right] r^2 \delta \, d\delta \, dz \, d\theta, \tag{7}$$

where η_s represents the atomic surface density of sphere of the three hydrogen atoms. Thus, the total potential energy for NH_3 interaction with an aquaporin is given by

$$V_{tot} = V_1 + V_2. \tag{8}$$

2.2 Nitric oxide molecule

Here, we obtain the interaction energy arising from the nitric oxide molecule interacting with two biological channels. We consider the nitrogen and oxygen as discrete atoms which are located on $(0, 0, z_0)$ and $(0, 0, z_0 - \sigma_f)$, respectively, interacting with an aquaporin (either GlpF or AQP1) as shown in Fig. 2. Thus, the total potential energy is given by

$$V_{tot} = \eta_c \int_{-\pi}^{\pi} \int_a^1 \left[\int_{-\frac{L}{2}}^{\frac{L}{2}} r^2 \delta(-A_N \rho^{-6} + B_N \rho^{-12}) \, dz + \int_{-\frac{L}{2}-\sigma_d}^{\frac{L}{2}-\sigma_d} r^2 \delta(-A_C \rho^{-6} + B_C \rho^{-12}) \, dz \right] d\delta \, d\theta, \tag{9}$$

where $\sigma_d = 1.685$ is the distance between the nitrogen and oxygen atoms.

3 Numerical results

In this section, we calculate the energies arising from the ammonia and nitric oxide molecules interacting with cylindrical aquaporin channels (GlpF and AQP1) and we obtain the plots of the total potential energy using MAPLE and MATLAB packages. The numerical values used in this paper are shown in Tables 1 and 2 where $N_G = 4{,}737$

Table 1 Lennard–Jones (ϵ and σ) constants [26,31,27,32]

Interaction	ϵ (eV $\times 10^{-2}$)	σ(Å)
H–H	0.190	2.886
N–H	1.032	3.273
N–N	1.296	3.660

Table 2 Physical parameters used in this paper [24]

Parameters	Symbol	Value
Length of aquaporin	L	28 Å
Outer radius of aquaporin	r_1	15 Å
Inner radius of aquaporin	r_0	12 Å
Radius of sphere of hydrogen atoms	b	1.296 Å
Distance between nitrogen and oxygen atoms	σ_d	1.15 Å
Volume density for GlpF	$\eta_c = [N_G / V_c]$	$[4{,}737/\pi Lr^2] = 0.3389$ atom/Å^3
Volume density for AQP1	$\eta_c = [N_Q / V_c]$	$[4{,}601/\pi Lr^2] = 0.3292$ atom/Å^3
Atomic surface density for a sphere of hydrogen	$\eta_s = 3/A_s$	0.1895 atom/Å^2
Channel wall thickness	$a = r_0^*/r_0$	0.25

and $N_Q = 4{,}601$ [24] are the number of atoms in the chemical compositions of GlpF and AQP1 channels, respectively. V_c is the volume of cylinder aquaporin and A_s is the surface area of sphere of the three hydrogen atoms. The attractive constants A and repulsive constants B are calculated by finding the well-depth ϵ and van der Waals diameter σ for all interaction pairs as shown in Table 3 [26,31].

Figures 4, 5, 6 and 7 show the total interaction energy of ammonia and nitric oxide molecules inside GlpF and AQP1 channels. We determine these interactions by two different approaches, namely numerical and computational methods. Firstly, we perform integrations over the volume unit to evaluate the numerical solution using the MAPLE package to evaluate integral as in Eqs. (6) and (7). Secondly, we refer to the infinite summation formulation as the computational solution. We need only evaluate the infinite summation to the first 10 terms for the solution to converge. Comparison between the two approaches confirms that the numerical and computational approaches are in good agreement.

Figure 4 shows the potential energy arising from the ammonia molecules (comprising the nitrogen atom and the hydrogen sphere) interacting with the aquaporin channel GlpF along the z-axis between $z_0 = -30$ Å and $z_0 = 30$ Å. We comment that there is minimal difference between the numerical and the computational results. We also note that the total interaction energy is practically zero at $z_0 = \pm 30$ Å and has minimum value of approximately -7.66 eV for a single ammonia molecule at the centre of the GlpF channel. Figure 4 also shows that the contribution from the nitrogen atom-GlpF and the hydrogen sphere-GlpF interaction at the origin are approximately -4.17 and -3.49 eV, respectively. From the Fig. 3, we can see that there is no energy barrier to inhibit the encapsulation of an ammonia molecule inside the GlpF channel.

In Fig. 5, we show the same interaction for the AQP1 channel and the results for the ammonia-AQP1 interaction are very similar to those of ammonia-GlpF. The total interaction energy at the centre of the AQP1 is approximately -7.62 eV. We comment that the corresponding minimum energy for the nitrogen atom-AQP1 and the hydrogen sphere-AQP1 interactions are approximately -4.06 and -3.56 eV.

Table 3 Numerical values of the attractive (A) and repulsive (B) constants taken from [26,31]

Element	Symbol	Value (eV Å^6)	Symbol	Value (eV Å$^{12} \times 10^3$)
OO	A_{OO}	22.63	B_{OO}	41.599
OH	A_{OH}	9.41	B_{OH}	9.972
OS	A_{OS}	79.89	B_{OS}	228.279
ON	A_{ON}	23.41	B_{ON}	49.283
OC	A_{OC}	33.79	B_{OC}	83.240
HH	A_{HH}	4.41	B_{HH}	2.548
HS	A_{HS}	41.10	B_{HS}	70.517
HN	A_{HN}	11.70	B_{HN}	14.383
HC	A_{HC}	17.16	B_{HC}	52.046
CN	A_{CN}	41.26	B_{CN}	115.661
CS	A_{CS}	139.04	B_{CS}	522.516
SN	A_{SN}	97.11	B_{SN}	314.772
CC	A_{CC}	58.71	B_{CC}	191.493
NN	A_{NN}	28.74	B_{NN}	69.083
SS	A_{SS}	324.72	B_{SS}	1401.426
N-GlpF	A_N	22.52	B_N	50.640
H-GlpF	A_H	8.92	B_H	17.734
O-GlpF	A_O	18.43	B_O	36.335
N-AQP1	A_N	22.55	B_N	50.482
H-AQP1	A_H	9.07	B_H	17.747
O-AQP1	A_O	18.82	B_O	36.901
NO-GlpF	A_{NO}	20.47	B_{NO}	43.487
NO-AQP1	A	20.68	B	43.691
NH_3-GlpF	A	12.32	B	25.960
NH_3-AQP1	A	12.44	B	25.931

From Figs. 6 and 7, We see that the potential energies for both interactions are practically zero at $z_0 \leq -30$ Å and $z_0 \geq 30$ Å and there is minimal difference between the computational and the numerical results for the whole range of values of z-axis. The results of NO-GlpF interaction due to the contribution of the N-GlpF and O-GlpF interaction pairs has a minimum energy of approximately -8.02 eV at the very centre of the GlpF while the NO-AQP1 interaction reaches its minimum value of mostly -7.86 eV. We also note that nitric oxide molecule would be freely accepted into both of the channels under consideration. These interactions have take the minimum value for the interaction energy at the centre of the channel due to this location leads to an optimum distance from the mass of the aquaporin to maximize the attractive van der Waals interaction. For the two channels considered here, the interaction of NO-GlpF is more favourable which is primarily due to the pore diameter difference between the two channels. We also note that for the range of parameters examined here, the computational and numerical solutions computed using MAPLE, the results

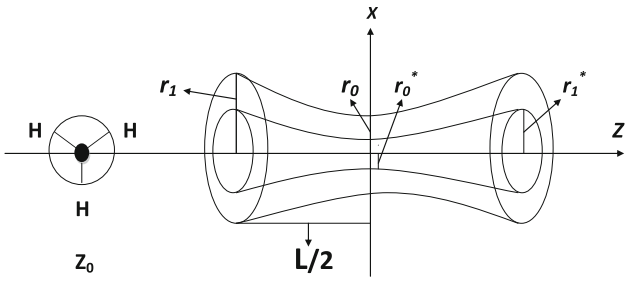

Fig. 3 Geometry of an ammonia molecule on z-axis interacting with an aquaporin assumed to be a flaired right cylinder

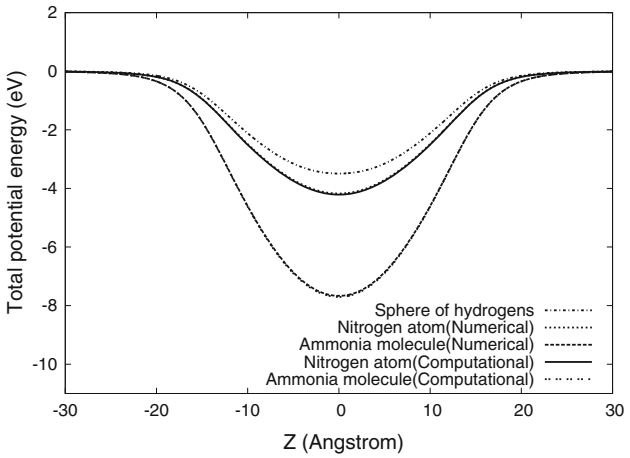

Fig. 4 Total potential energy for nitrogen atom, sphere of hydrogen atoms and ammonia molecule on the z-axis interacting with GlpF

are almost identical provided that at least the first 10 terms are evaluated from the infinite summation.

Our results show the acceptance of NH_3 inside the GlpF and AQP1 channels is satisfied and elucidate the crucial role of the aquaporin inner radius r_0 in determining the magnitude of the maximum interaction energy due to the channel narrowing in the middle of the aquaporin. We comment that the NH_3 molecule is accepted into these channels with having very small activation barrier inside the AQP1 channel. This is also in very good agreement with the recent studies, such as Kruse et. al. [17] confirmed that the GlpF and AQP1 can facilitate the conductance of NH_3 gas through membranes of these channels. In addition, the reference interaction site model theory predicts that nitric oxide, urea and glycerol can only pass through the GlpF channel, due to there being a large barrier in the PMF at the selective filter region in AQP1 and all these molecules have negative PMF throughout the AQP1 channel but the ammonia gas has very small energetic barriers in AQP1 channel. Furthermore, the work of Verkman [20] indicates that small gas molecules transported by proteins should not be ignored. These results are also in agreement with

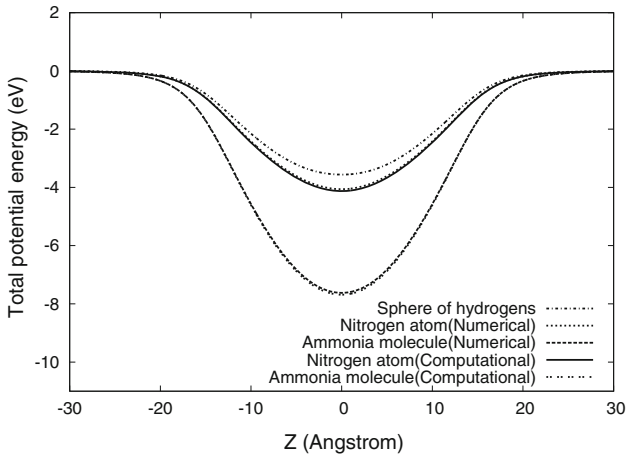

Fig. 5 Total potential energy for nitrogen atom, sphere of hydrogen atoms and ammonia molecule on the z-axis interacting with AQP1

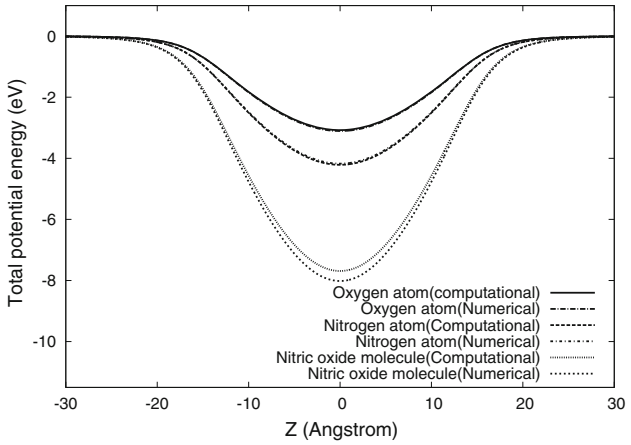

Fig. 6 Total potential energy for nitrogen and oxygen as discrete atoms and and nitric oxide molecule on the z-axis interacting with GlpF

Phongphanphanee et al. [6], who reported that ammonia molecule can be permeated through the AQP1 and GlpF channels, this is because AQP1 channel has only a small activation barrier to be overcome [6] and recently the transportation of NH_3 has been verified with evidences that AQP1 can transport the NH_3 molecule through its membrane [6,16]. The minimum energies, arising from the interaction between the ammonia and water molecules, and AQP1 and GlpF channels, are constrained between $z_0 = -20\,\text{Å}$ and $z_0 = 20\,\text{Å}$ while the local minimum energy in the middle of the aquaporin channel (around $z_0 = 0\,\text{Å}$) [16,18]. Yi et al. [33], indicate that gas permeation through AQPs is variant and the average of normal rate of gas permeation through the central pore (in the middle of AQP1) of being roughly 4.6 kcal/mol energy barrier in the periplasmic vestibule. Further, The work of Herrera

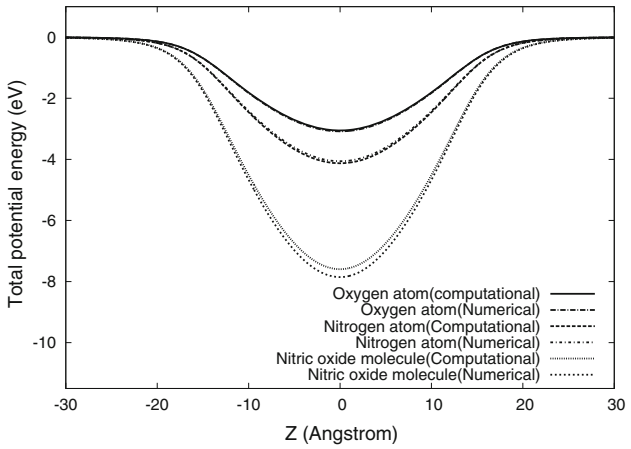

Fig. 7 Total potential energy for nitrogen and oxygen as discrete atoms and and nitric oxide molecule on the z-axis interacting with AQP1

et al. [21] who determine the flux rate of NO through AQP1 which is approximately 7.0 ± 0.9 units/s and it occurs under the physiological conditions and correlated with osmotic permeability. Nakhoul et al. [22] and Holbrook and Zwieniecki [23] who have shown that the water channel AQP-1 are able to transport small gas molecules, such as carbon dioxide, nitric oxide and ammonia in through cell membrane protein.

4 Summary

In this paper, we present a mathematical model which explains the biological mechanism of ammonia and nitric oxide molecules entering aquaporin channels. This model investigates and describes the interaction between NH_3 and NO molecules and flaired right cylindrical aquaporin channels which are assumed to have a gradual change in the radius r in the shape of a parabolic curve. The van der Waals interaction energy is calculated using the six-twelve Lennard-Jones potential, assuming the chemical compositions of the GlpF and AQP1 channels to be $C_{1289}H_{2527}N_{315}O_{591}S_{11}$ and $C_{1235}H_{2468}N_{320}O_{601}S_7$, respectively. For the ammonia molecule, we apply the discrete-continuum approach for the nitrogen atom as an arbitrary point on the z-axis and a sphere of the three hydrogen atoms interacting with a flaired right cylindrical GlpF and AQP1. We then find the total potential energy for these interactions. Further, the interaction of nitric oxide with two aquaporin channels modelled in two parts: the nitrogen and oxygen as discrete points interacting with GlpF and AQP1 channels. We find that the aquaporin radius r plays a significant role in determining the minimum and maximum energy for these interactions. Our results indicate the acceptance of the ammonia and nitric oxide molecules being encapsulated into the interior of these channels. Our calculations are in good agreement with Kruse et al. [17], Verkman [20], the Polymer Reference Interaction Site Model (3D-RISM theory) and the statistical mechanics theory of molecular liquids [6,18].

Acknowledgments The authors are grateful to the Australian Research Council for support through the Discovery project scheme and for the provision of an APD for BJC. They are also grateful to the provision of an UPA for HA.

References

1. A.S. Verkman, K.A. Mitra, Structure and function of aquaporin water channels. Am. J. Physiol. Renal Physiol. **278**, 13–28 (2000)
2. K. Murata, K. Mitsouka, T. Hirai, T. Walz, P. Agre, J.B. Heymann, A. Engel, Y. Fujiyoshi, Structural determinants of water permeation through aquaporin-1. Nature **407**, 599–605 (2000)
3. G. Ren, V.S. Reddy, A. Cheng, P. Mylnek, A.K. Mitra, Three-dimensional fold of the human aqp1 water channel determined at 4Å resolution by electron crystallography of two-dimensional crystals embedded in ice. J. Mol. Biol. **301**, 369–387 (2000)
4. D. Fu, A. Libson, L.J.W. Miercke, C. Weitzman, P. Nollert, J. Krucinski, R.M. Stroud, Structure of a glycerol-conducting channel and the basis for its selectivity. Science **290**, 481–486 (2000)
5. G.M. Preston, T.P. Carrol, W.B. Guggino, P. Agre, Appearance of water channels in xenopus oocytes expressing red cell CHIP28 water channel. Science **256**, 385–387 (1992)
6. S. Phongphanphanee, N. Yoshida, F. Hirata, Molecular selectivity in aquaporin channels studied by the 3D-RISM theory. J. Phys. Chem. B **114**, 7967–7973 (2010)
7. M.O. Jensen, S. Park, K. Schulten, E. Tajkhorshid, and ed. by L.D. Donald, Energetics of glycerol conduction through aquaglyceroporin GlpF. Proc. Natl. Acad. Sci. **99**, 6731–6736 (2002)
8. J.M. Verbavats, D. Brown, I. Sabolic, G. Valenti, D.A. Siello, A.N. Van Hoek, T. Ma, A.S. Verkman, Tetrameric assembly of CHIP28 water channels in liposomes and cell membranes: a freeze-fracture study. Cell Biology **123**, 605–618 (1993)
9. J.S. Jung, G.M. Preston, B.L. Smith, W.B. Guggino, P. Agre, Molecular structure of the water channel through aquaporin CHIP. The hourglass model. J. Biol. Chem. **269**, 14648–14654 (1994)
10. G.M. Pao, L.F. Wu, K.D. Johnson, H. Hofte, M.J. Crispeels, G. Sweet, N.N. Sandal, M. Sauer, Evolution of the mip family of integral membrane transport proteins. Mol. Microbiol. **5**, 33–37 (1991)
11. G.J. Wistow, M.M. Pisano, A.B. Chepelinsky, Tandem sequence repeats in transmembrane channel proteins. Trend Biol. Sci. **16**, 170–171 (1991)
12. G.M. Preston, J.S. Jung, W.B. Guggino, P. Agre, Membrane topology of aquaporin chip. Analysis of functional epitope-scanning mutants by vectorial proteolysis. J. Biol. Chem. **269**, 1668–1673 (1994)
13. B.L. Smith, P. Agre, Erythrocyte mr 28,000 transmembrane protein exists as a multisubunit oligomer similar to channel proteins. J. Biol. Chem. **266**, 6407–6415 (1991)
14. K.B. Heller, E.C. Lin, T.H. Wilson, Substrate specificity and transport properties of the glycerol facilitator of escherichia coli. Bacteriol **144**, 274–278 (1980)
15. G. Ren, V.S. Reddy, A. Cheng, A.K. Mitra, Visualization of a water-selective pore by electron crystallography in vitreous ice. Proc. Natl. Acad. Sci. **98**, 1398–1403 (2001)
16. J.S. Hub, L.B. de Groot, Comment on "molecular selectivity in aquaporin channels studied by the 3D-RISM theory". J. Phys. Chem. B **115**, 8364–8366 (2011)
17. E. Kruse, N. Uehlein, R. Kaldenhoff, The aquaporins. Genome Biol. J. **7**(2), 206–211 (2006)
18. J.S. Hub, L.B. de Groot, Mechanism of selectivity in aquaporins and aquaglyceroporins. Proc. Natl. Acad. Sci. USA **105**, 1198–1203 (2008)
19. Y.C. Hou, A. Janczuk, P.G. Wang, Current trends in the development of nitric oxide donors. Current Pharm. Des. **5**(6), 417–441 (1999)
20. A.S. Verkman, Does aquaporin-1 pass gas? An opposing view. J. Physiol. **542**, 31 (2002)
21. M. Herrera, N.J. Hong, J.L. Garvin, Aquaporin-1 transports NO across cell membranes. Hypertension **48**, 157–164 (2006)
22. N.L. Nakhoul, K.S. Hering-Smith, S.M. Abdulnour-Nakhoul, L.L. Hamm, Transport of NH_3/NH in oocytes expressing aquaporin-1. Am. J. Physiol.-Renal Fluid Electrol. Physiol. **281**, 255–263 (2001)
23. N.M. Holbrook, M.A. Zwieniecki, Plant biology: water gate. Nature **425**, 361 (2003)
24. D.F. Savage, P.F. Egea, C.Y. Robles, J.D. O'Conell III, and R.M. Stroud, Architecture and selectivity in aquaporins 2.5 Å x-ray structure of aquaporin Z. Public Libr. Sci. Biol. **1**, 334–340 (2003)
25. J.O. Hirschfelder, C.F. Curtiss, R.B. Byron, The molecular theory of gases and liquids. Society For Industrial and Applied Mathematics, NewYork, University of Winsconsin, Madison, 1964
26. L.T. Cottrell, *The Strengths of Chemical Bonds* (Butterworths, London, 1954)

27. L. Pauling, *The Nature of the Chemical Bonds* (Cornell University Press, Ithaca, NY, 1960)
28. L.A. Girifalco, M. Hodak, R.S. Lee, Carbon nanotube, buckyballs, ropes and a universal graphitic potential. Phys. Rev. Lett. **62**, 104–110 (2000)
29. H. Al Garalleh, N. Thamwattana, B.J. Cox, J.M. Hill, Modelling van der waals interaction between water molecules and biological channels. J. Comput. Theor. Nanosci. **10**, 1–10 (2013)
30. B.J. Cox, N. Thamwattana, J.M. Hill, Mechanics of atoms and fullerenes in single-walled carbon nanotubes, in *Proceedings of The Royal Society A*, vol. 463 (The Royal Society, 2006), pp. 461–476
31. L.E. Sutton, Table of interatomic distances and configuration in molecules and ions. (Chemical Society, London, 1965)
32. A.K. Rappi, C.J. Casewit, K.S. Colwell, W.M. Skid, UFF, a full periodic table force field for molecular mechanics and molecular dynamics simulations. J. Am. Chem. Soc. **114**, 10024–10035 (1992)
33. Y. Wang, J. Cohen, W.F. Boron, K. Schulten, E. Tajkhorshid, Exploring gas permeability of cellular membranes and membrane channels with molecular dynamics. J. Struct. Biol. **157**, 534 –544 (2007)